

DIELECTRIC MULTIPACTOR DISCHARGES AT 110 GHz

S. C. Schaub*, M. A. Shapiro, R. J. Temkin,
Massachusetts Institute of Technology, Cambridge, MA, USA

Abstract

A 1.5 MW, 110 GHz gyrotron has been used to experimentally measure the maximum sustainable fields on dielectric materials in vacuum. The purpose of this work is to evaluate the suitability of these materials for future applications in high frequency linear accelerators and high power terahertz components. To our knowledge, these are the first measurements of multipactor phenomena in the millimeter wave or terahertz frequency range. Materials tested include alumina, sapphire, fused quartz, crystal quartz, and high resistivity silicon. Dielectric samples were tested both as windows, with electric fields parallel to the surface, and sub-wavelength dielectric rod waveguides, with electric fields perpendicular to the surface. Visible light emission, absorbed/scattered microwave power, and emitted electrons were measured to characterize the discharges on the dielectric surfaces. The results of these experiments are compared to theoretical calculations of multipactor discharges, testing these models at significantly higher frequencies than has been done before.

INTRODUCTION

Research has begun to test the feasibility of RF linear accelerators operating at W-band frequencies and above (>100 GHz) [1, 2]. At MIT, we are experimentally testing breakdown limits of materials and cavities subject to intense W-band RF, in high vacuum conditions (10^{-8} Torr). Presented here are the results of ongoing research of multipactor discharges on dielectric surfaces.

EXPERIMENT DESIGN

High power microwaves are provided by a 1.5 MW, 110 GHz gyrotron that provides 3 microsecond pulses at a rate of 1 Hz [3]. The output of this gyrotron is a Gaussian beam, coupled into a highly overmoded, corrugated waveguide for transport to a test structure. Two separate test geometries have been developed to study multipactor discharges with 110 GHz electric fields perpendicular to, or parallel to the surfaces of the materials under study. Test structures were designed to generate surface fields in excess of 100 MV/m with 1 MW of input power, while avoiding triple points (vacuum, metal, and dielectric intersections) in regions with non-negligible fields. In addition, the structures were designed to have open configurations that would allow the use of optical diagnostics and dark current probes to characterize the discharges.

Perpendicular E Configuration

A dielectric rod-waveguide configuration was constructed to allow testing of multipactor breakdown thresholds with

the RF E-field perpendicular to the surface of the sample. In this configuration, the incoming Gaussian beam is focused to a 1.5 mm spot size onto the end of a sub-wavelength ($0.18-0.29 \lambda$ diameter) rod. Approximately 90% of the incident beam power couples to the HE_{11} mode of the dielectric rod waveguide. The rods are thin enough that only a single mode is confined at the test frequency. The dielectric rod is the sample under test, and the diameter of each rod is chosen to maximize the surface field of the confined mode. The test geometry is illustrated in Fig. 1.

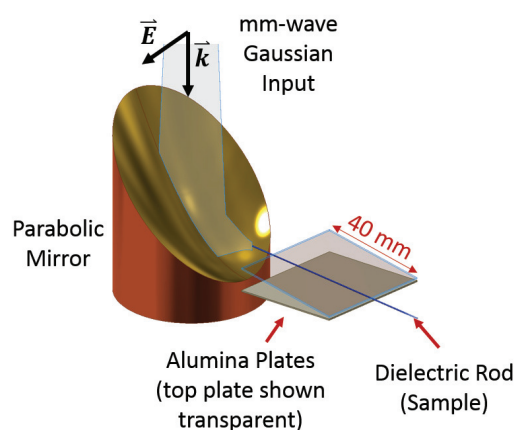


Figure 1: CAD drawing of perpendicular E-field dielectric testing configuration. The upper alumina plate is drawn transparent for clarity.

In our experiment, the HE_{11} mode of a sub-wavelength, solid dielectric waveguide concentrates the electric fields on the sides of the rod (in the direction of polarization) and the magnetic field on the top and bottom surfaces of the rod. To provide further field enhancement, alumina plates form a taper above and below the rod. On the side away from the rod, these plates are metalized, to interact with and cutoff the magnetic field of the HE_{11} mode, while minimally perturbing the structure of the electric field on the sides of the rod. The RF electric and magnetic fields of this system were calculated in ANSYS HFSS, and are shown in Fig. 2. A 1 MW Gaussian beam is incident on the left end of the dielectric rod in simulation. The taper cuts off the mode near the right end of the rod, setting up a standing wave and generating peak surface fields in excess of 120 MV/m.

Parallel E Configuration

A second configuration has been constructed to allow testing of multipactor breakdown thresholds with the RF E-field parallel to the surface of the sample. Shown in Fig. 3, a Fabry-Perot resonator was used to confine a Gaussian beam mode. Two $\lambda/4$ thick, 25.4 mm diameter silicon wafers,

* sschaub@mit.edu

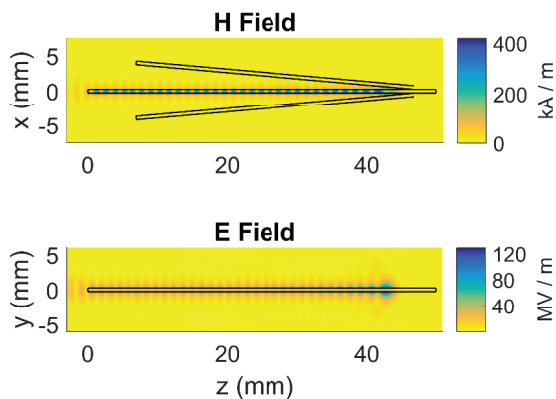


Figure 2: Complex magnitude of the H-fields and E-fields in the perpendicular E-field dielectric testing configuration. The upper and lower views are orthogonal planes. The peak E-field is 120 MV/m and the peak H-field is 400 kA/m for 1 MW of power incident from the left.

separated by 0.9 mm, form a semi-transparent mirror, onto which a Gaussian beam is focused. The other end of the cavity is formed by a 11.1 mm radius spherical copper mirror. This mirror is mounted on a piezoelectric actuator to allow for tuning of the resonant cavity frequency. All components of this cavity were supported in a stainless steel threaded lens tube, to provide stability to the cavity dimensions. The sides of the lens tube were cut away to allow for diagnostics and vacuum pumping.

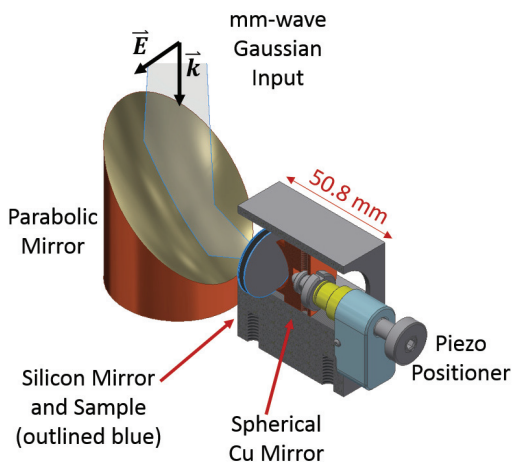


Figure 3: CAD drawing of parallel E-field dielectric testing configuration. The dielectric mirror and sample under test are outlined in blue.

The electric field in the test cavity is shown in Fig. 4 with a fused quartz sample. The sample is placed at the second field maximum within the cavity. 1 MW of power incident on the semi-transparent mirror yields surface fields of 145 MV/m on the sample.

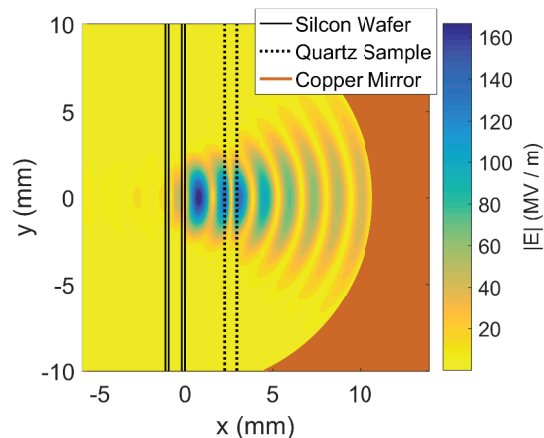


Figure 4: The standing wave E-field strength is shown for 1 MW of 110 GHz power incident from the left and passing through the two silicon wafers (acting as a partially transmitting mirror); the quartz sample (under test); and reflecting from the copper mirror (acting as a retroreflector). The surface field on the sample peaks at 145 MV/m.

HIGH POWER TESTING

High power testing has been performed on alumina, sapphire, and fused quartz samples in both test configurations. The sapphire samples were a c-axis rod, and a c-axis wafer, so that electric fields were largely perpendicular to the optical axis of the samples tested. Visible light, dark current probes, and reflected power diagnostics were used to detect multipactor discharges. Visible light patterns are seen in Fig. 5. In the perpendicular E-field test, a standing wave structure is clearly seen on the rod, and matches well with the simulated E-field pattern. In the parallel E-field test, a symmetric glow is centered on the test disk.

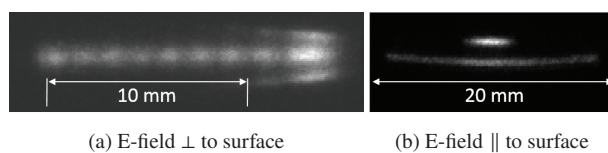


Figure 5: Black and white visible light images of multipactor discharges on a) a sapphire rod and b) a sapphire disk (seen nearly on edge). The E-field is polarized out of the page in both images.

Example forward and reverse RF power and dark current traces are shown for each test structure in Figs. 6 and 7. In the non-resonant, perpendicular E-field test structure, Fig. 6, the multipactor discharge absorbs a significant portion of the RF power.

Fig. 7 shows two example shots from the Fabry-Perot configuration. Fig. 7a) shows a low power shot with no discharge and b) displays a higher power shot with a multipactor discharge. Between the two shots, the cavity length was slightly adjusted, so that, in Fig. 7b), the cavity was on resonance after the multipactor discharge had formed on the

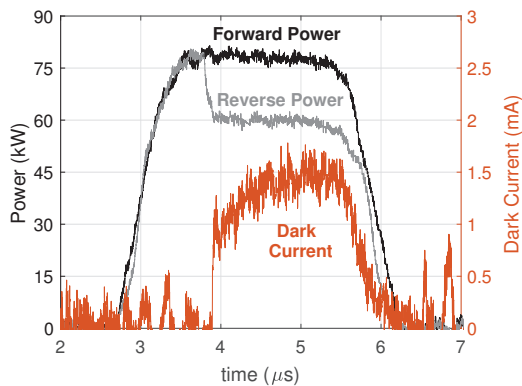


Figure 6: Power and dark current traces from the dielectric rod configuration with a discharge at 3.9 microseconds.

sample. This was done to accurately measure the change in the coupling coefficient of the cavity, and indirectly measure the power absorbed by the multipactor discharge.

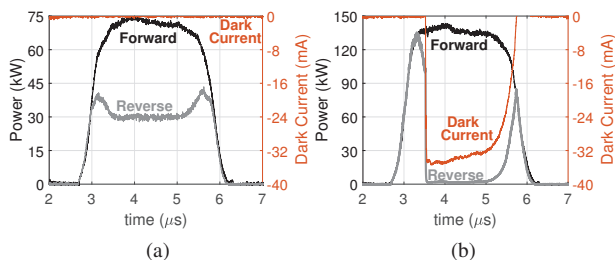


Figure 7: Power and dark current traces from the Fabry-Perot configuration. No discharge exists in (a). A discharge forms at 3.5 microseconds in (b).

CURRENT RESULTS

All samples tested, with the exception of the fused quartz with parallel E-field, were subjected to at least 150k shots for processing. In multiple tests, the fused quartz disks were damaged after a small number of multipactor discharges. Measured threshold surface fields for multipactor are in Table 1.

Table 1: Multipactor Thresholds

Material	E-field	Calculated	Measured
Sapphire	⊥	35 MV/m	26 MV/m
Sapphire	∥	42 MV/m	40 MV/m
99.8% Alumina	⊥	35 MV/m	26 MV/m
99.9% Alumina	∥	28 MV/m	17 MV/m
Fused Quartz	⊥	In Progress	31 MV/m
Fused Quartz	∥	53 MV/m	44 MV/m

The calculated thresholds in Table 1 are the preliminary results of ongoing Monte Carlo calculations. The perpendicular E-field configuration is modeled in one dimension,

including the radial dependence of the electric fields. The parallel E-field configuration is modeled in two dimensions, as it is necessary to include the influence of the RF magnetic field to approach agreement with both historical, lower frequency and current experimental results. These calculations are still being refined and benchmarked.

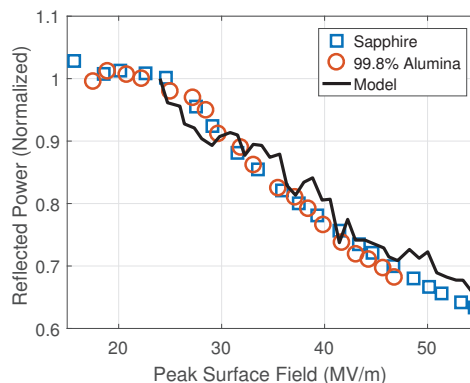


Figure 8: Power absorbed by multipactor on sapphire and alumina rods, compared with the results of a Monte Carlo calculation

In addition to predicting multipactor thresholds, the Monte Carlo calculations in development are being used to model the power absorption that has been experimentally measured. The early results in Fig. 8 show excellent agreement with the data for alumina and sapphire with perpendicular surface E-fields.

FUTURE WORK

With the parallel E-field test structure, additional high power testing will be performed on samples of crystal quartz and high-resistivity silicon. This will broaden the range of material parameters studied, allowing a more thorough comparison between experiment and numerical models. Additionally, the calculations currently in progress will be further refined and expanded to all materials tested.

ACKNOWLEDGMENTS

This work is supported by the U.S. Department of Energy High Energy Physics grant number DE-SC0015566.

REFERENCES

- [1] M. Dal Forno *et al.*, “Experimental measurements of rf breakdowns and deflecting gradients in mm-wave metallic accelerating structures,” *Phys. Rev. Accel. Beams*, **19**, 051302, (2016).
- [2] E. A. Nanni *et al.*, “Prototyping high-gradient mm-wave accelerating structures,” *J. Phys.: Conf Ser.* **874**, 012039, (2017).
- [3] D. S. Tax *et al.*, “Experimental Results on a 1.5 MW, 110 GHz Gyrotron with a Smooth Mirror Mode Converter,” *J. Infrared, Millimeter, Terahertz Waves* **32**, 358, (2011).